

This article was downloaded by: [University of Haifa Library]

On: 13 August 2012, At: 20:40

Publisher: Taylor & Francis

Informa Ltd Registered in England and Wales Registered Number: 1072954 Registered office: Mortimer House, 37-41 Mortimer Street, London W1T 3JH, UK



## Molecular Crystals and Liquid Crystals

Publication details, including instructions for authors and subscription information:

<http://www.tandfonline.com/loi/gmcl20>

### Exploration of Size Effects in Cylindrical Nematic Samples: A Numerical Simulation and ESR Study

Alexandre E. Gomes<sup>a</sup>, Antonino Polimeno<sup>a</sup>, Assis F. Martins<sup>b</sup>, Stefano Ceola<sup>a</sup> & Carlo Corvaja<sup>a</sup>

<sup>a</sup> Dipartimento di Chimica Fisica, Università degli Studi di Padova, Via Loredan 2, Padova, 35131, Italy

<sup>b</sup> Departamento de Ciência dos Materiais, FCT, Universidade Nova de Lisboa, Monte de Caparica, 2825-114, Portugal

Version of record first published: 29 Oct 2010

To cite this article: Alexandre E. Gomes, Antonino Polimeno, Assis F. Martins, Stefano Ceola & Carlo Corvaja (2002): Exploration of Size Effects in Cylindrical Nematic Samples: A Numerical Simulation and ESR Study, *Molecular Crystals and Liquid Crystals*, 372:1, 135-143

To link to this article: <http://dx.doi.org/10.1080/713738171>

PLEASE SCROLL DOWN FOR ARTICLE

Full terms and conditions of use: <http://www.tandfonline.com/page/terms-and-conditions>

This article may be used for research, teaching, and private study purposes. Any substantial or systematic reproduction, redistribution, reselling, loan, sub-licensing, systematic supply, or distribution in any form to anyone is expressly forbidden.

The publisher does not give any warranty express or implied or make any representation that the contents will be complete or accurate or up to date. The accuracy of any instructions, formulae, and drug doses should be independently verified with primary sources. The publisher shall not be liable for any loss, actions, claims, proceedings, demand, or costs or damages whatsoever or howsoever caused arising directly or indirectly in connection with or arising out of the use of this material.

## Exploration of Size Effects in Cylindrical Nematic Samples: A Numerical Simulation and ESR Study

ALEXANDRE. E. GOMES<sup>a</sup>, ANTONINO POLIMENO<sup>a</sup>,  
ASSIS F. MARTINS<sup>b</sup>, STEFANO CEOLA<sup>a</sup>  
and CARLO CORVAJA<sup>a</sup>

<sup>a</sup>*Dipartimento di Chimica Fisica, Università degli Studi di Padova,  
Via Loredan 2, 35131 Padova, Italy and*

<sup>b</sup>*Departamento de Ciência dos Materiais, FCT, Universidade Nova de Lisboa,  
2825-114 Monte de Caparica, Portugal*

**Abstract** A numerical treatment is developed and implemented to solve the constitutive equations of nematodynamics according to the Leslie-Ericksen formulation for a cylindrical geometry. Nematic director equations in three dimensions are coupled to a Navier-Stokes description of the velocity. This model is used to study the influence of the sample size for an experimental set-up corresponding to an combined electron spin resonance (ESR) rheological experiment in which the nematic sample is subject to a constant rotational velocity and to an aligning magnetic field perpendicular to the axis of rotation. The results of the simulations are employed to interpret experimental findings for a series of measurements of the ESR signal of tempone-<sup>14</sup>N dissolved in capillaries of different sizes containing the nematic liquid crystal ZLI 1083, with diameters ranging from 0.1 to 0.5 mm.

**Keywords** nematic liquid crystals; Leslie-Ericksen equations; rheology of complex fluids; electron spin resonance spectra

## INTRODUCTION

Flow properties of nematic liquid crystalline phases are described by Leslie-Ericksen equations<sup>[1,2]</sup>:

$$\left[ \hat{\mathbf{V}} \cdot \boldsymbol{\sigma} \right] = \rho \frac{dv}{dt} \quad (1)$$

$$\mathbf{G} + \mathbf{g} + \left[ \hat{\mathbf{V}} \cdot \boldsymbol{\pi} \right] = 0 \quad (2)$$

Equation (1) describes the time evolution of the velocity field  $v(\mathbf{r}, t)$  in a point  $\mathbf{r}$  of the nematic at time  $t$ . Tensor  $\boldsymbol{\sigma}$  represents the stress tensor of the material;  $\rho$  is the bulk density. Equation (2) defines the properties of the unitary vector  $\mathbf{n}(\mathbf{r}, t)$ , i.e. the liquid crystal director field. Here  $\mathbf{G}$  represents the external force acting on the director, i.e. the perturbation to the system induced by external fields, e.g. magnetic or electric fields, while  $\mathbf{g}$  is the internal body force, i.e. the term responsible for director time rearrangement due to direct coupling with the velocity flow; the last contribution describes the elastic force resulting from coupling with elastic tensor  $\boldsymbol{\pi}$ . The stress tensor  $\boldsymbol{\sigma}$  elements can be written as a linear combination of terms depending of the components of the velocity and director fields and their derivatives as well as of the six viscosity coefficients  $\alpha_i$ ,  $i=1, \dots, 6$ , known as Leslie coefficients. Both the stress tensor and the internal force field depend on the elastic energy  $W$ , which is dependent on the director components and elastic constants  $K_{11}$ ,  $K_{22}$ ,  $K_{33}$ :

$$W = \frac{1}{2} K_{11} \left( \hat{\mathbf{V}} \cdot \mathbf{n} \right)^2 + \frac{1}{2} K_{22} \left( \mathbf{n} \cdot \hat{\mathbf{V}} \times \mathbf{n} \right)^2 + \frac{1}{2} K_{33} \left( \mathbf{n} \times \hat{\mathbf{V}} \times \mathbf{n} \right)^2 \quad (3)$$

A complete numerical treatment of Leslie-Ericksen (LE) Eqns. (1) and (2)<sup>[3,4]</sup> is difficult: the intrinsic complication of the non-linear equations is enhanced by the necessity of solving for quantities  $\mathbf{n}$  and  $\mathbf{v}$  subject to constraints of unitary modulus and incompressibility, respectively. Without dealing with technical details, we shall present in this work a preliminary report of an approximate numerical treatment especially devised to treat curvilinear, in our case cylindrical, geometries, in three dimensions. Results will be presented to interpret a set of continuous rotation experiments performed on nematics in

cylindrical vessels, under the influence of a magnetic field, in a combined rheological and electron spin resonance experiment (Rheo-ESR)<sup>[5,6,7]</sup>. A number of simplifying assumptions have been introduced to allow a fast numerical solution. First of all the spherical approximation to Frank's elastic constants ( $K_{11}=K_{22}=K_{33}=K$ ) is used. In this case the expression for the elastic energy is reduced to:  

$$W = \frac{1}{2} K n_{i,j} n_{i,j}$$

Next LE equations have been simplified by assuming that in the specific experimental conditions the explicit dependence upon the spatial coordinate in the  $z$ -axis direction is negligible. Essentially a translational invariance has been introduced by assuming an infinitely long test tube. Strong anchoring boundary conditions were employed to describe the behavior of the nematic material at the container wall.

Moreover, the velocity field  $\mathbf{v}$  has been treated according to a Navier-Stokes description: in other words, the director influence on the velocity flow behavior in Eq. (2) is neglected. The resulting set of equations is amenable to a full computational approach, which is based on a finite difference discretization in a polar grid of points defined in the  $xy$  plane; time is treated through an accurate, explicit scheme.

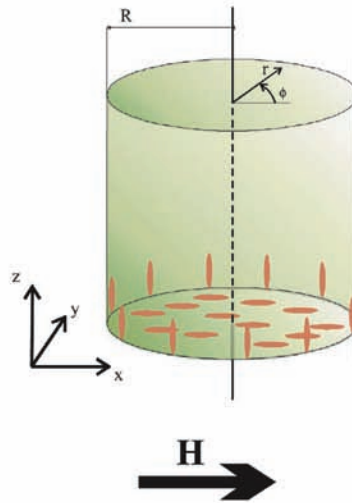


FIGURE 1 Sample geometry and initial director configuration

## EXPERIMENTAL CONDITIONS

We shall discuss a set of results related to continuous wave ESR measurements (CW-ESR) performed on nematic ZLI 1083 in cylindrical containers with diameters ranging from 0.1 mm to 0.3 mm (i.e.  $R=0.05$  to 0.15 mm, see Figure 1) and subjected to a continuous rotation at a constant rotational velocity  $\Omega$  ranging from 0 to 0.25 Hz. The experiment was carried out by measuring the ESR spectrum of  $^{14}\text{N}$ -tempone dissolved in the liquid crystal sample. The solution was placed into a capillary tube in turn inserted into a larger tube to allow a better stability of spinning: a Teflon support was used to hold the internal tube, containing the sample, fixed with respect to the external tube along its axis.

The time-dependent EPR signal was collected at room temperature, 298 K, well inside the nematic mesomorphic region of ZLI 1083. A computer controlled one-step motor was employed for spinning the sample. An optical switch, made up of a reflecting disc with a radial cleft integrated in the motor shaft and an infrared led with a photodiode, assured the synchronization of the ER-200 SH spectrometer with the motor. The sample was initially left still in the spectrometer magnetic field  $H=3361.5$  G for some time (1-2 hours). Initial conditions immediately before starting to spin the sample were assumed of perfect alignment of the nematic director with the magnetic field.

## SIMULATION RESULTS

Simulations were performed by choosing strong anchoring boundary conditions for the director field along the tube axis, and perfect adherence of the fluid flow. The internal walls of the cylinder are then assumed, for sake of simplicity, i) to align the director along the  $z$ -direction and ii) to transfer momentum to the flow, i.e. the fluid velocity at the walls is equal to the cylinder rotational velocity. All the physical constants employed in the simulations (magnetic susceptibility, Leslie's viscosities and Frank's elastic constants) are reported in Table 1

Density (g.cm <sup>-3</sup> )	1
Magnetic susceptibility	1x10 <sup>-7</sup>
Leslie Viscosities	-0.115; -0.115; -0.28;
$\alpha_1$ ; $\alpha_2$ ; $\alpha_3$ ; $\alpha_4$ ; $\alpha_5$ ; $\alpha_6$ (Poise)	0.28; 0.115; -0.28
Frank's Elastic Constants	5.3; 2.2; 7.45
$K_{11}$ ; $K_{22}$ ; $K_{33}$ (x10 <sup>-6</sup> dyne)	

TABLE 1 Viscoelastic parameters used in the simulated experiment

The spatial grid ( $\sim 10^3$  points) and time step ( $10^{-4}$  s) employed in all simulations were chosen to assure a satisfactory numerical resolution and an affordable computational time, which is typically of 24-48 hours on a parallel machine of 8 processors.

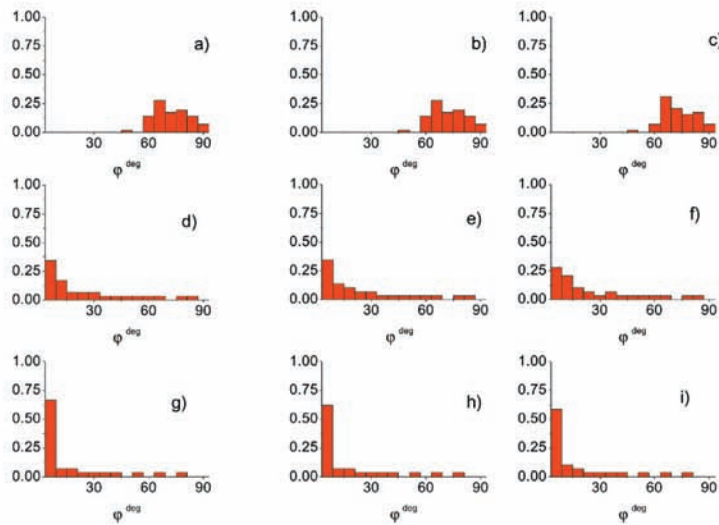


FIGURE 2 Distributions of the local director orientation for:  
R = 0.05mm, a)  $\Omega = 0.05$  Hz; b)  $\Omega = 0.15$  Hz; c)  $\Omega = 0.25$  Hz;  
R = 0.10mm, d)  $\Omega = 0.05$  Hz ; e)  $\Omega = 0.15$  Hz ; f)  $\Omega = 0.25$  Hz;  
R = 0.15mm, g)  $\Omega = 0.05$  Hz ; h)  $\Omega = 0.15$  Hz ; i)  $\Omega = 0.25$  Hz

Results are presented in Figure 2 in the form of histograms of the director orientation distribution at the final time of the simulation for

some of the most representative rotational velocities. The stationary configuration, that is the stationary pattern assumed by the director under the competing magnetic and mechanical torque is in practice independent of the rotational velocity (horizontal axis). A strong dependence is however observed with respect to the radius of the sample (vertical axis), as a consequence of the strong anchoring boundary conditions: this effect is especially evident for the smaller sample radius.

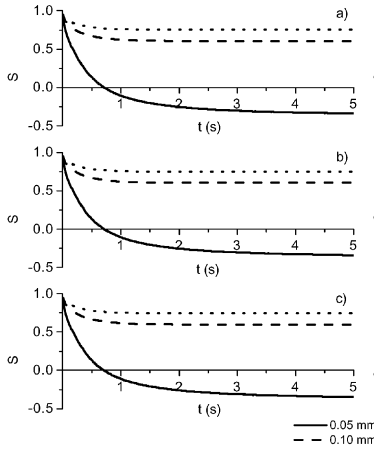


FIGURE 3 Plot of the time evolution of order parameter  $S$  for different velocities: a) 0.05 Hz; b) 0.15 Hz; c) 0.25 Hz

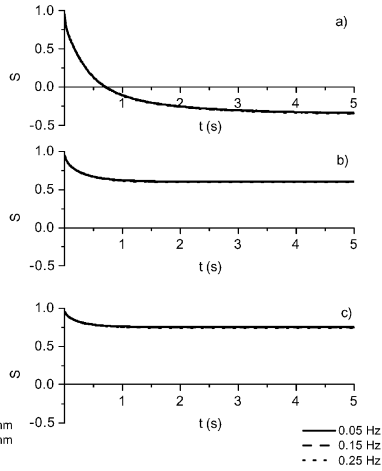


FIGURE 4 Plot of the time evolution of the order parameter  $S$  for different radii: a) 0.05 mm; b) 0.10 mm; c) 0.15 mm

In Figures 3 and 4 we show the time evolution of the average quantity  $S = \langle (3 \cos^2 \varphi - 1) \rangle / 2$ , where  $\varphi$  is the angle formed by the director with the magnetic field direction and  $\langle \dots \rangle$  indicates the average in the whole sample, for different velocities, Figure 3, and radii, Figure 4: again a strong influence of the sample size but a negligible influence of the rotational velocity is evident. To better understand the pattern assumed by the director in the sample, in Figure 5 we show the initial and final 3D snapshots of the director orientation in the sample for different radii. The director local configuration is represented in an orthogonal perspective by an ensemble of rods, one for each grid point.

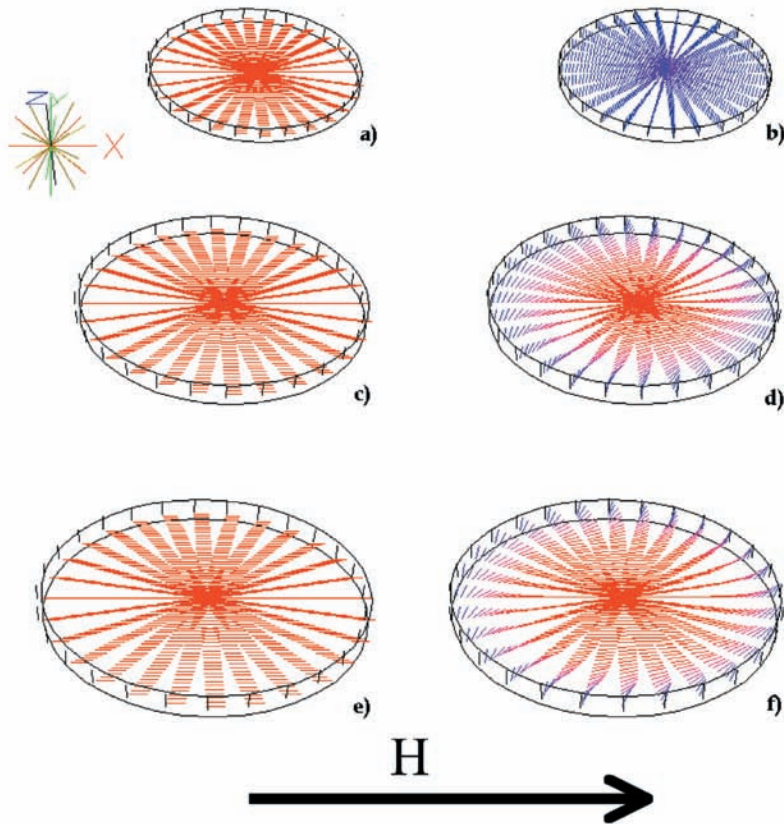


FIGURE 5 3D snapshots of the director configuration,  $\Omega=0.5$  Hz:  
 $R = 0.10$  mm, a)  $t=0$ ; b)  $t=5$  s ;  $R = 0.20$  mm, c)  $t=0$ ; d)  $t=5$  s ;  $R = 0.25$  mm, e)  $t=0$  ; f)  $t=5$  s.

Finally in Figure 6 a) we show the experimental director distribution obtained experimentally, by analyzing the ESR spectrum once stationary conditions are reached, for a non-spinning sample. It was obtained from the high field hyperfine component of the EPR spectra. The first derivative line was integrated and then deconvoluted with a line shape obtained from the central line of the nitroxide contained in a tube of larger diameter. The assumption was made that



the line width does not change with the orientation of the director. The high field line was chosen for the analysis since the position of this line is the most affected by molecular movement.

In Figure 6 b) the calculated histograms obtained from simulations are shown. The qualitative agreement of experimental and simulated results is satisfactory, and a number of features observed are effectively reproduced by the simulations: the nematic exhibits at small radii a relevant region of alignment with the internal walls, as manifested by the contribution to the measured distribution around 90 degrees; for larger samples the alignment with the magnetic field predominates (the distribution is peaked around 0 degrees). The agreement with simulation is acceptable, since this behavior with increasing size is reproduced. However, we can observe that in general simulations tend to overestimate the aligning effect of the boundaries: perfect strong anchoring is clearly not realistic and should be considered as a simplified description of the actual interface between the nematic and the internal walls of the tube. Also, a better estimate of viscoelastic parameter would be in order to better compare the result of the hydrodynamical calculations with available experimental data.

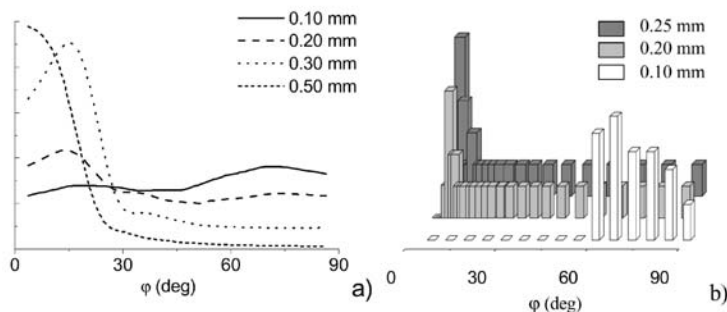


FIGURE 6 a) Experimental director orientation for a stationary sample with different sample radius. b) Simulated Director orientation for a stationary sample with different sample radius.

## CONCLUSIONS

In this work an interpretation of experimental findings on nematic samples in cylindrical containers studied by CW-ESR, in still conditions and subjected to constant spinning, was presented. Experimental results presented here were by necessity limited to a small fraction of the available data, and we have shown only distributions of the director obtained from ESR spectra of non-spinning sample, and the corresponding simulations. For the case of spinning samples, we have shown how the size effects are dominant in determining the stationary distribution of the director, whereas the magnitude of spinning is less important, at least for the slow spinning case presented here.

## ACKNOWLEDGEMENTS

We thank professor G.J. Moro for valuable and stimulating discussions.

We acknowledge the financial support of the E.C. TMR Contract N. FMRX-CT97-0121.

## References

- <sup>[1]</sup> F. L. Leslie, Quart. J. Mech. Appl. Math., **19**, 357 (1966); Adv. Liq. Cryst., **4**, 1 (1979).
- <sup>[2]</sup> J.L. Ericksen, Trans. Soc. Rheolo., **5**, 23 (1961); Adv. Liq Cryst., **2**, 233 (1976)
- <sup>[3]</sup> A. Polimeno and A.F. Martins, Liq. Cryst., **25**, 545 (1998)
- <sup>[4]</sup> A. Polimeno, L. Orian, A. E. Gomes and A. F. Martins, Phys. Rev. E., **62**, 2, 2288 (2000)
- <sup>[5]</sup> F.M. Leslie, G.R. Luckhurst and H.J. Smith, Chem. Phys. Lett., **13**, 368 (1972)
- <sup>[6]</sup> J.W. Emsley, S. K. Khoo, J. C. Lindon and G.R. Luckhurst, Chem. Phys. Lett., **77**, 609 (1981)
- <sup>[7]</sup> C. J. Dunn, D. Ionescu, N. Kunimatsu, G. R. Luckhurst, L. Orian, A. Polimeno, J. Phys. B, **47**, 104, 10989 (2000)